Liquid-surface entrainment induced by a planar shock wave

Vincent Rodriguez, Georges Jourdan, A. Marty, A. Allou, J.-D. Parisse

Noname manuscript No.
(will be inserted by the editor)

Liquid-surface entrainment induced by a planar shock wave

V. Rodriguez · G. Jourdan · A. Marty · A. Allou · J.-D. Parisse

Received: date / Accepted: date

Abstract Recently, we experimentally studied, in shock tube environment, shock waves sliding over horizontal free water layers having depths of 10 mm, 20 mm, and 30 mm for shock wave Mach numbers M_{is} respectively equal to 1.1 and 1.4. The qualitative interaction process was observed by means of a high-speed visualizations and arising pressures in the air and in the water layer were measured and interpreted in terms of the various incident and refracted shock waves in air and water; in particular it was concluded that the compression wave in the water is driven by the planar shock wave in the air. Additional experiments have been conducted and the novel contributions of the present technical note are quantitative results about the liquid-surface entrainment. At low Mach number (M_{is}=1.1), we show that the velocity of the droplets ejected into the air is independent of the water depth, unlike the wavelength of initial ripples and the angle of ejection. When the shock wave strength increases (M_{is}=1.4) the dispersion of a very thin droplet mist and a single large wave take place. We show that the thickening of the water mist and the velocity of the subsequent large wave decreases with the water-layer depth.

Keywords Experiments · shock wave · air-water interface · droplet dispersion

E-mail: vincent.rodriguez@ensma.fr
V. Rodriguez* · G. Jourdan · A. Marty
Aix-Marseille Université, IUSTI, UMR CNRS 7343, Marseille, France.
*Present address: Institut Pprime, UPR CNRS 3346, ENSMA, 86961 Futuroscope-Chasseneuil Cedex, France.
A. Allou
CEA, DEN, Cadarache, DTN/STCP/LTRS, 13108 Saint Paul lez Durance Cedex, France.
J.-D. Parisse
French Air Force Academy, Salon de Provence, BA701, 13661 Salon Air.

1 Introduction

The processes by which liquid layers are stripped and re-entrained into the gas stream are complex and still require fundamental investigations and specifically in unsteady airstreams. Even if this problem may occur as a natural phenomenon as well as in a number of technical applications, only few works are available in the literature especially for shock-induced flow [1–3]. In order to study the snatching of liquid layers induced by gas stream, shock waves at low Mach numbers (M_{is}= 1.1 and 1.4) have been used to initiate the flow over water layer. Experiments were performed at atmospheric pressure and room temperature in the T200 large square cross section shock tube of IUSTI (200×200 mm^2) for a 1500-mm-long water surface. Details of the design of the experimental set-up have been already presented in previous articles [4,5]. High-speed visualization paths both normal and angled at 45° to the flow were used in order to obtain improved examination of the process details. Surface wave formation and specific patterns according to the shock strength were distinctly observed. In parallel, detailed pressure mapping, analyzed both in the water and the air, pointed out that the underwater compression wave does not move at the water speed of sound but it is driven by the propagation of the shock wave in air to ensure the continuity of the pressure at the air-water interface. After qualitatively describing the phenomenology of the interaction in our previous study [4], we conducted additional experiments in order to extract the most representative quantities of the process whose evolution could be useful for the validation of future models and numerical simulations. For the three depths studied, we determined the wavelength of the roll waves generated at the air-liquid interface, the trajectories and the angle

of ejection of the macroscopic droplets detached by gas stream for the experiments conducted at Mach number M_{is}=1.1. For stronger shock wave Mach number experiments (M_{is}=1.4), the temporal evolutions of the fine mist thickness and the motion of the traveling single wave could be determined from experimental data.

2 Results and discussions

A series of snapshots of the air-water interface is displayed in Fig. 1 and illustrates the interaction of an incident shock wave of Mach number M_{is}=1.11 with a water-layer depth of 10 mm. In the present case, after the shock wave passage, the air is set in motion at approximatively 60 m/s and starts to destabilize the liquid surface leading to the growth of roll waves in accordance with the Kelvin-Helmholtz instability phenomenon. Specifically the picture of Fig. 1(d) allows to evaluate the distance λ between each rolls numbered from 1 to 8. The wavelength of the ripples has been estimated to 4.5 mm in the present case but for the water-layer depth of 20 mm and 30 mm, the wavelength increases to 5.4 mm and 7.5 mm, respectively. However, from the classical theory of Kelvin-Helmholtz instability [6,7], in presence of density gradient $\nabla\rho = \rho_{water} - \rho_{air}$ and surface tension η, the wavenumber k of the first wave to go unstable is $k = \sqrt{\frac{g\nabla\rho}{\eta}}$ and the air flow velocity necessary to drive waves at the air-water interface can be calculated by $U = \sqrt{\frac{\rho_{water}+\rho_{air}}{\rho_{water}\rho_{air}}(\eta k + \frac{g}{k}\nabla\rho)}$ If we put $g = 9.8$, $\rho_{water} = 1000$, $\rho_{air} = 1.25$ and $\eta = 0.074$ appropriate for air above water, we find the critical wavelength of the waves $2\pi/k = 1.7$ cm travelling at velocity $U = 6.6$ m/s. Conversely, applying the same theory, for air blowing over water at 60 m/s, the wavelength of the disturbances should be of about 0.1 mm which is not in agreement with experimental observations. It is clear that Kelvin-Helmholtz instability alone can not explain the physical process with sufficient precision for high speed flow induced by shock waves. Note that it was more difficult to determine the wavelength of the ripples for experiments conducted at Mach number M_{is}=1.43 because of both the dense water-mist which hides them and the insufficient image resolution. Indeed, when the Mach number increases the wavelength of the perturbations decreases. Approximately, it was evaluated five times smaller than that obtained at Mach 1.11. Afterwards, the wave crest forms a thin liquid film that flaps as the wave grows downstream. In our case where the gas speed is great enough, we can observed that the film breaks up into droplets which are eventually thrown into the gas stream with an angle whose evolutions are presented in Fig. 2. We

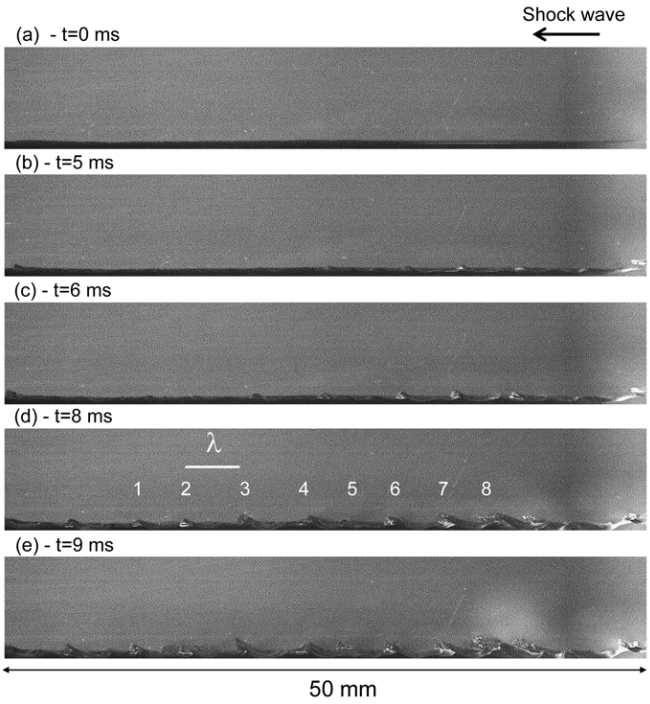

Fig. 1 Sequence of pictures showing the interaction of an incident shock wave of Mach number M_{is}=1.11 with a layer of water 10 mm deep. λ represents the distance between each rolls numbered from 1 to 8.

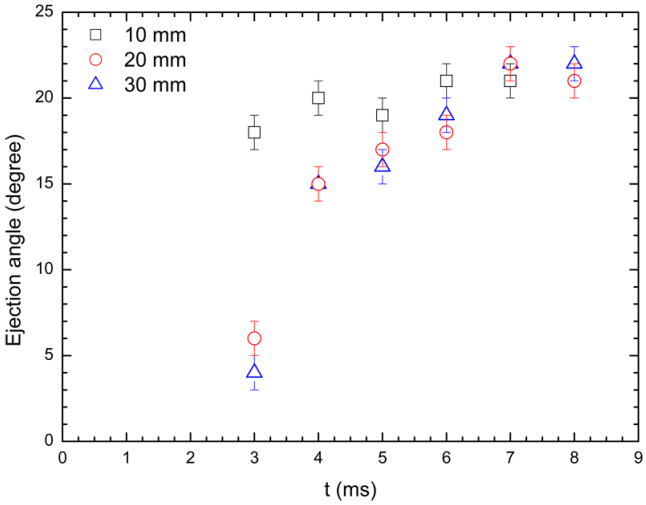

Fig. 2 Time dependence of the angle of ejection of droplet mist induced by shocked air flow for three depths of water. The incident shock-wave Mach number M_{is}=1.11.

measured the angle of ejection by carefully observing at the beginning of the water layer individual ejection events. We carried out measurements for three water depths at fixed air velocity induced by shock-wave Mach number M_{is}=1.11. If at early time the angle of ejection differs, probably due to unsteady flow induced by different shock wave refraction scenarii according to the liquid layer depth, when the flow is uniformly

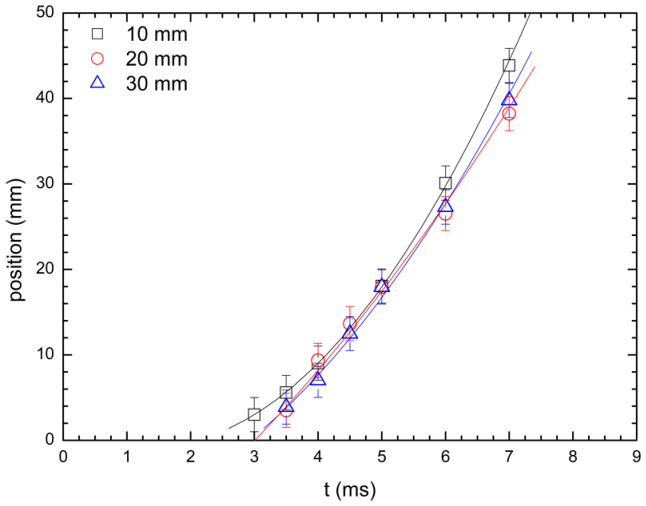

Fig. 3 Motion of traveling droplets induced by shocked air flow for three depths of water. The incident shock-wave Mach number M_{is}=1.11.

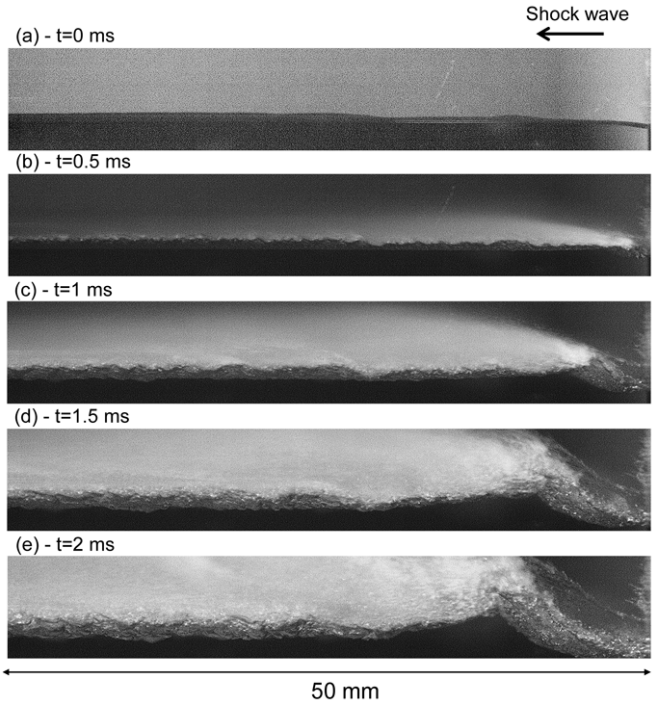

Fig. 4 Sequence of pictures showing the interaction of an incident shock wave of Mach number M_{is}=1.43 with a layer of water 20 mm deep.

established the angle reaches to the same asymptotic value of 23° for the three water-layer depths. Once ejected into the air stream, motion of the droplets is observed and Fig. 3 presents their trajectory as a function of time for the 1.11-shock-wave Mach number and for three water-layer depths. As we can see, the graph presents three parabolic trajectories almost identical regardless of the initial depth of water probably governed by droplet dynamics under the influence of flow nonuniformity and relative acceleration . After derivation, the mean velocity can be deduced and it is estimated in the present case of about 10 m/s. Fig. 4 presents a series of pictures showing the interaction of an incident shock wave of Mach number M_{is}=1.43 with a layer of water 20 mm deep. Following the shock front (not visible on pictures) we can observe smaller water ripples as said above which are induced by the shocked air flowing at 200 m/s (Fig. 4(b)). As the flow progresses over the surface, a single largeamplitude wave is formed. The photographs also show the dynamics of water fog entrainment into the shock induced air flow. In this case, the spray is formed from the entire water surface shortly after the passage of the shock wave and grows in thickness in time. The most representative quantities that can be extracted from our experiments are the thickening of the fine mist ripped from the water surface and the displacement of the single wave. Figure 5 presents the time dependence of the thickness of mist layer induced by shocked air flow for three initial water-layer depths at three different distances from the beginning of the liquid layer. It is clear that the deeper the water layer, the thinner the water mist. Moreover, the growth rate of the water-mist thickness decreases with distance from the beginning of the water layer. Thereafter, the main feature we subsequently observe is a steadily-propagating single large wave whose location can be determined as a function of time from the passage of the initial shock front over the beginning of the liquid layer. Figure 6 presents the trajectories for the three water-layer depths and indicates that the deeper the water layer, the slower the wave moves: for a shock wave Mach number M_{is}=1.43 the single wave is moving at velocities of 8.96 m/s, 8.15 m/s and 4.87 m/s for depths of 10, 20 and 30 mm, repectively. This result is consistent with the fact that the wave is apparently driven by the force resulting from the stagnation of the flow just downstream of the step where the mass of water is accumulated.

3 Conclusion

We have experimentally studied the dispersion of a water layer by the flow induced by a shock wave (shock Mach numbers M_{is}=1.11 and 1.43) sliding over a water layer having depths of 10 mm, 20 mm, and 30 mm. According to the incident shock wave strength, the features observed at the air-water interface are different and the most representative quantities experimentally accesible are also different. For experiments conducted with shock wave Mach number M_{is}=1.1 our results

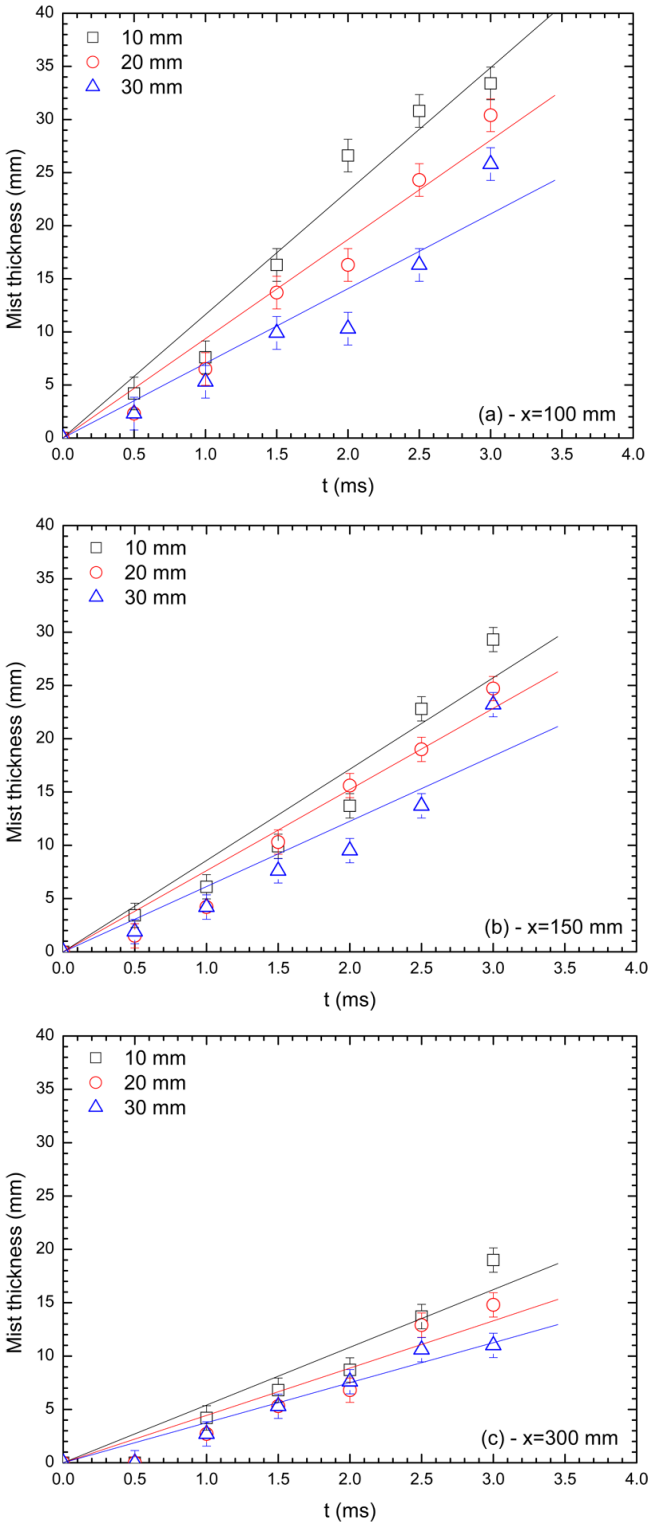

Fig. 5 Time dependence of the thickness of mist layer induced by shocked air flow at three locations: (a) x=100 mm, (b) x=150 mm and (c) x=300 mm from the beginning of the water layer. The incident shock-wave Mach number M_{is}=1.43.

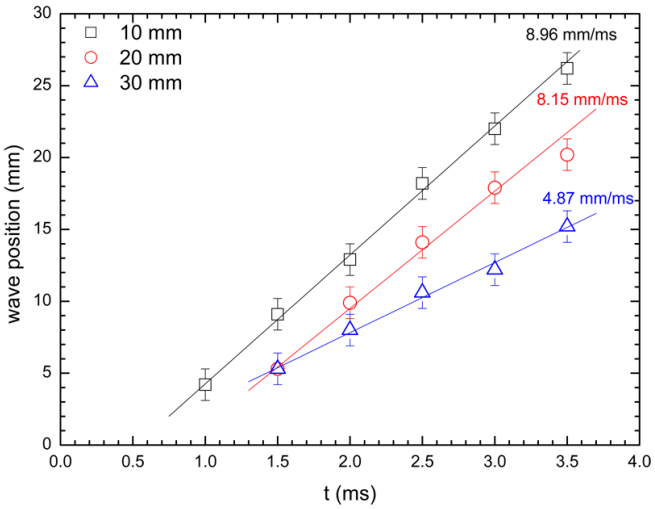

Fig. 6 Motion of traveling wave induced by shocked air flow for three depths of water. The incident shock-wave Mach number M_{is}=1.43.

show that the water depth influences the wavelength of initial ripples and the angle of ejection of the droplets ejected into the air. But their entrainment in the air flow seems to be independent of the depth. When the shock wave strength increases (M_{is}=1.4) we show that the thickening of the water mist and the velocity of the subsequent large wave decreases with the water-layer depth. An important point however have to be raised. If the Kelvin-Helmholtz instability involves in the destabilization of the layer of water, it does not fully explain the present results. Now, for Mach numbers and depths gradually varying, further experiments have to be conducted, not focusing only on the gas-liquid interface, in order to connect the flow resulting from the shock diffraction on the water surface with its ensuing destabilization and entrainment. However, the unsteady two-phase aspect in presence of shock of the phenomenon makes its diagnosis, with usual techniques (direct illumination, schlieren methods or plane-laser scattering), limited.

Acknowledgements

This work is supported by CEA Cadarache under Contract #4000649074 CJN-001.

References

1. Borisov A. A., Kogarko S. M., Lyubimov A. V., Sliding of detonation and shock waves over liquid surfaces, Combustion, Explosions and Shock Waves, vol 1, 31-38 (1965)
2. Milton B.E., Behnia M., Takayama K., Interaction of liquid films with shock induced airflows, Proceedings of the

18th International Symposium on Shock Waves Held at Sendai Japan, vol 2, 1265-1270 (1991)
3. Teodorczyk A., Shepherd J. E., Interaction of a shock wave with a water layer, Technical Report No. FM2012-002, Graduate Aeronautical Laboratories, California Institute of Technology, Revision of December 2015.
4. Rodriguez V., Jourdan G., Marty A., Allou A., Parisse J.-D., Planar shock wave sliding over a water layer, Experiments in Fluids, 57:125 (2016)
5. Houas L., Jourdan G., Schwaederlé L., Carrey R., Diaz F., A new large cross-section shock tube for studies of turbulent mixing induced by interfacial hydrodynamic instability, Shock Waves, vol 13, 431-434 (2003)
6. Jerome J.J.S., Marty S., Matas J.-P., Zaleski S., Hoepffner J., Vortices catapult droplets in atomization, Phys. Fluids, 112109 (2013)
7. Knotek S., Jicha M., Introduction to liquid wall film atomization, EPJ Web of Conferences 25, 02011 (2012)